DEUTSCHES ELEKTRONEN-SYNCHROTRON

DESY 93-197
December 1993

Lepton-Nucleon Scattering at High Energies

W. Buchmüller
Deutsches Elektronen-Synchrotron DESY, Hamburg

ISSN 0418-9833

NOTKESTRASSE 85 - 22603 HAMBURG

To be sure that your preprints are promptly included in the
HIGH ENERGY PHYSICS INDEX,
send them to (if possible by air mail):

DESY **Bibliothek** **Notkestraße 85** **22603 Hamburg** **Germany**	**DESY-IfH** **Bibliothek** **Platanenallee 6** **15738 Zeuthen** **Germany**

DESY 93-197
December 1993

ISSN 0418-9833

LEPTON-NUCLEON SCATTERING AT HIGH ENERGIES *

W. BUCHMÜLLER
Deutsches Elektronen-Synchrotron DESY
Hamburg, Germany

ABSTRACT

Recent theoretical developments in the field of inelastic lepton-nucleon scattering are reviewed with emphasis on physics at HERA. Structure functions at small Bjorken-x are discussed in detail. Further topics are photoproduction of jets, the gluon densities in proton and photon, charm physics, electroweak processes and the search for new particles and interactions.

Structure Functions

Inelastic lepton-nucleon scattering is characterized by three kinematical variables, the total center-of-mass energy s, the invariant momentum transfer Q^2 and Bjorken's scaling variable x. They read in terms of the four-momenta of the scattering process (cf. fig. (1)),

$$s = (k+P)^2 \ , \quad Q^2 = -q^2 \ , \quad x = \frac{Q^2}{2\nu} \ , \qquad (1)$$

where $\nu = P \cdot q$. Different experiments differ in the range in x and Q^2 which they can probe. In the past fixed target experiments have studied the domain $x > 0.01$, $Q^2 < 300$ GeV^2. At HERA this kinematic region has been extended by two orders of magnitude in each direction down to $x > 10^{-4}$ and up to $Q^2 < 3 \cdot 10^4$ GeV^2. Hopefully, in the future a further extension by one order of magnitude in x and Q^2 will be achieved at LEP⊗LHC.

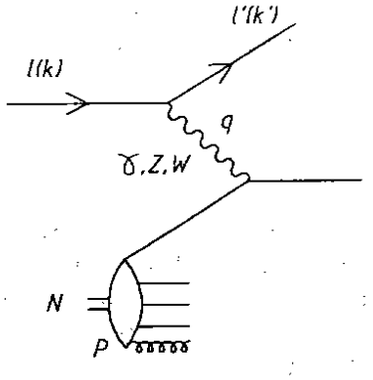

Figure 1: Inelastic lepton-nucleon scattering

What is the prediction of Quantum Chromodynamics (QCD), the theory of strong interactions, for inelastic lepton-nucleon scattering? Let us briefly recall the basic theoretical ideas (cf., e.g., [1,2]). The inclusive cross section is obtained by summing over all final states X. In the case of one-photon exchange it takes the form

$$d\sigma(lN) = \sum_X d\sigma(lN \to l'X) \propto L_{\mu\nu} W^{\mu\nu} \ . \qquad (2)$$

Here $L_{\mu\nu}$ is the well know leptonic tensor, and the hadronic tensor $W_{\mu\nu}$ is determined by the two structure functions F_1 and F_2,

$$W_{\mu\nu}(P,q) = \left(-g_{\mu\nu} + \frac{q_\mu q_\nu}{q^2}\right) F_1(x,Q^2) + \frac{1}{\nu}\left(P_\mu - \frac{\nu}{q^2}q_\mu\right)\left(P_\nu - \frac{\nu}{q^2}q_\nu\right) F_2(x,Q^2) \ . \qquad (3)$$

One of the most important predictions of QCD is the occurence of scaling in the Bjorken limit $\nu, Q^2 \to \infty$ with $x = Q^2/2\nu$ fixed, broken by logarithmic deviations. In the Bjorken limit the hadronic tensor is dominated by the light-cone and can be calculated using the operator product expansion. For moments of structure functions one obtains,

$$M_{2,J}(Q^2) \equiv \int_0^1 dx x^{J-2} F_2(x,Q^2) = \sum_i A_J^i(\mu^2) C_{2,J}^i\left(\frac{Q^2}{\mu^2}, g^2\right) \ . \qquad (4)$$

Here the first factor of the product is given by the non-perturbative "reduced" matrix element $< N|O_i^J|N >$ of an operator with spin J, whereas the coefficient function $C_{2,J}^i$ can be calculated in perturbation theory. Splitting the structure functions in a flavour singlet and a flavour non-singlet part, $F_2(x,Q^2) = F_2^S(x,Q^2) + F_2^{NS}(x,Q^2)$, the Q^2-evolution of the non-singlet moments is determined by the simple equation

$$Q^2 \frac{d}{Q^2} M_{2,J}^{NS}(Q^2) = \alpha(Q^2)\gamma_J M_{2,J}^{NS}(Q^2) \ , \qquad (5)$$

where γ_J is the anomalous dimension of the operator O^J. Due to asymptotic freedom, i.e., $\alpha_s(Q^2) \propto$

*Talk given at the Europhysics Conference on High Energy Physics, Marseille, July 1993

$1/b_0 \ln Q^2/\Lambda^2$ for $Q^2 \gg \Lambda^2$, one obtains for the non-singlet moments at large Q^2

$$M_{2,J}^{NS}(Q^2) \propto \left(\frac{1}{\ln \frac{Q^2}{\Lambda^2}}\right)^{-4\pi\gamma_J/b_0} . \quad (6)$$

This equation yields the logarithmic deviations from scaling in terms of QCD parameters.

Under certain assumptions on the analytic properties of the structure functions (cf. [1,2]), eqs. (5) for all spins J are equivalent to the evolution equation of the structure function

$$Q^2 \frac{\partial}{\partial Q^2} F_2^{NS}(x,Q^2) = \frac{\alpha_s(Q^2)}{2\pi} \int_x^1 \frac{dx'}{x'} P_{qq}\left(\frac{x}{x'}\right) F_2^{NS}(x',Q^2) . \quad (7)$$

P_{qq} is the quark-quark Altarelli-Parisi splitting function [3] whose moments are proportinal to the anomalous dimensions, $\int_0^1 dx x^{J-1} P_{qq}(x) \propto \gamma_J$. The evolution equation (7) has an intuitive interpretation in the QCD-improved parton model, where $P_{qq}(x/x')$ is the probability for a quark with momentum fraction x' to split into a quark with momentum fraction $x < x'$ and a gluon with momentum fraction $x' - x$. The structure function can then be expressed as a linear combination of densities $q(x,Q^2)$ of the respective quark species in an appropriate frame of reference, which is the infinite momentum frame. The Q^2-dependence of the parton densities is mostly due to gluon bremsstrahlung. The flavour-singlet part of the structure function $F_2^S(x,Q^2)$ mixes with the gluon density $g(x,Q^2)$, and the evolution equation therefore involves a 2x2 matrix of splitting functions. The entire system of evolution equations for structure functions and parton densities is frequently referred to as DGLAP equations [3-5].

So far we have discussed the "leading-twist" part of the operator product expansion in leading-order perturbation theory, which is equivalent to the QCD improved parton model. Present analyses include also next-to-leading order corrections for the leading-twist part and estimates of higher-twist contributions which are of relative order $1/Q^2$,

$$F_2(x,Q^2) = F_2^{LT}(x,Q^2) + \frac{1}{Q^2} F_2^{HT}(x,Q^2) , \quad (8)$$

where the connection between the leading-twist part F_2^{LT} and the parton densities depends on the renormalization scheme.

Theoretical prediction of scaling violations at large Q^2 can be compared with a variety of measurements of structure functions for neutral and charged current processes and of direct-photon production cross sections. New results reported at this conference have been summarized by Roberts [6]. Globel fits to all data have been performed by several groups [7-9]. All experimental results are consistent with the QCD predictions. As a result of their analysis Martin et al. [9] find for the strong coupling constant and the QCD scale parameter

$$\alpha_{\overline{MS}}(m_Z^2) = 0.112^{+0.004}_{-0.005} , \quad (9)$$

$$\Lambda^{(4)}_{\overline{MS}} = 230 \pm 55\text{MeV} . \quad (10)$$

At HERA the accessible range in x and Q^2 is extended by two orders of magnitude. This is apparent from fig. (2) where SLAC and BCDMS data on F_2 are compared with Monte Carlo data for HERA [10]. First

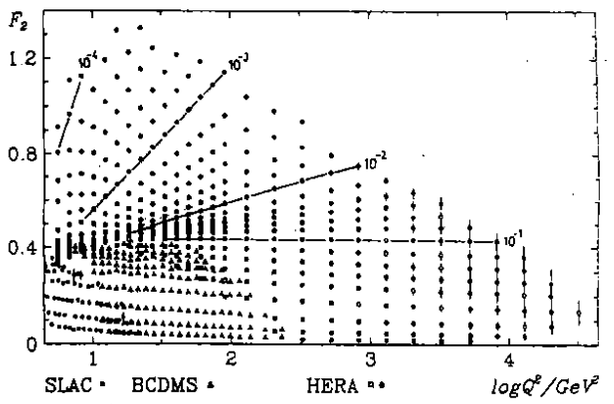

Figure 2: Monte Carlo data for F_2 as expected at HERA with an integrated luminosity of 100 pb^{-1}, compared with SLAC and BCDMS data. The x values are given in the figure. From [10].

results on scaling violations have been reported by the ZEUS collaboration [11]. Eventually, one hopes to reach a precision of about 50 MeV for the scale parameter $\Lambda_{\overline{MS}}$ [12]. Contrary to previous experiments, the strong coupling constant can be measured over a large range in Q^2 at HERA.

Structure Functions at Low x

New, interesting results on the structure function $F_2(x,Q^2)$ for values of x below 10^{-3} have been presented by the collaborations H1 and ZEUS for different values of Q^2 [13,14]. Data at two different values of Q^2 are shown in fig. (3).

What does QCD predict for the small-x behaviour* of parton densities? So far a rigorous analysis based

*Many interesting contributions to this subject can be found in the proceedings of two topical workshops, Nuclear Physics B (Proc. Suppl.) 18C (1990) and Journal of Physics G: Nuclear and Particle Physics 19 (1993).

on the operator product expansion, as discussed above for the large-Q^2 behaviour, has not been carried out. Almost all approaches to the small-x region extend the QCD improved parton model by including some infinite series of higher-twist contributions.

The DGLAP evolution equations imply that parton densities are shifted towards smaller values of x as Q^2 increases. For $x < 0.2$ the gluon density $g(x, Q^2)$ dominates over the quark densities. To understand the behaviour of all densities at very small values of x one can first study the evolution of the gluon density only,

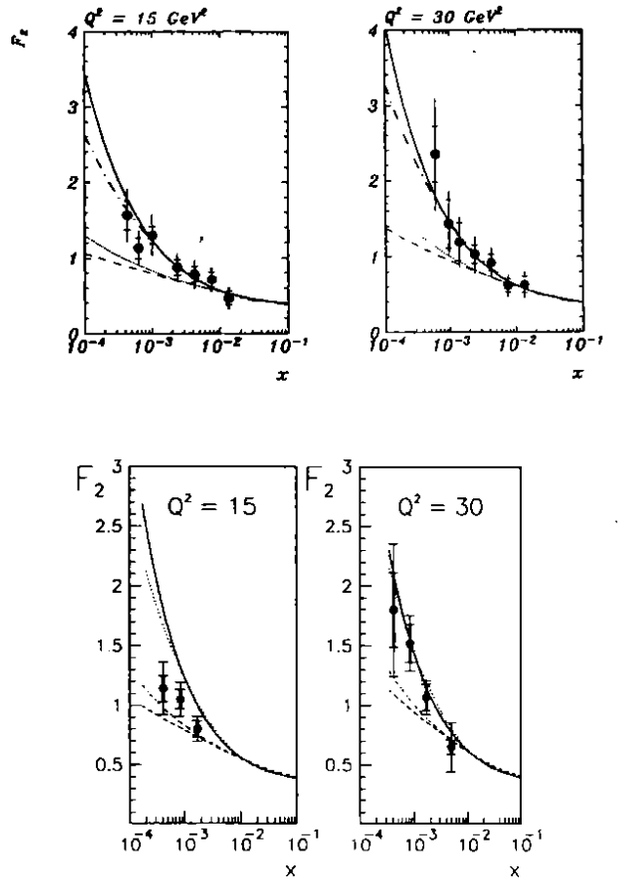

Figure 3: H1 (top) and Zeus (bottom) data for $F_2(x, Q^2)$ at $Q^2 = 15$ GeV^2 and $Q^2 = 30$ GeV^2.

as predicted by the pure gauge theory, which then acts as driving force for the quark sea. One has

$$Q^2 \frac{\partial}{\partial Q^2} g(x, Q^2) \approx \frac{\alpha(Q^2)}{2\pi} \int_x^1 \frac{dx'}{x'} P_{gg}(\frac{x}{x'}) g(x', Q^2) \; . \quad (11)$$

Since for small x, $P_{gg}(x/x') \approx 6\; x'/x$, one obtains the differential equation for the gluon density

$$\frac{\partial}{\partial \ln \frac{1}{x}} \frac{\partial}{\partial \ln \frac{Q^2}{\Lambda^2}} xg(x, Q^2) = \frac{12}{b_0 \ln \frac{Q^2}{\Lambda^2}} xg(x, Q^2) \; . \quad (12)$$

The solution

$$xg(x, Q^2) \sim \exp\left(\frac{48}{b_0} \ln \frac{\ln \frac{Q^2}{\Lambda^2}}{\ln \frac{Q_0^2}{\Lambda^2}} \ln \frac{1}{x} \right)^{1/2} \quad (13)$$

implies that $xg(x, Q^2)$ grows faster than any power of $\ln(\frac{1}{x})$ as $x \to 0$. Asymptotically, this cannot be correct since it would violate unitarity. However, eq. (13) may very well be a good approximation to the true gluon density in a certain range of x, which must depend on Q^2.

The growth of the gluon density at small x is due to gluon radiation, and eq. (13) can be obtained from

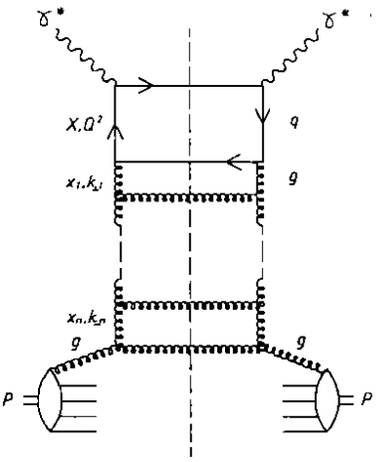

Figure 4: Ladder diagrams contributing to $F_2(x, Q^2)$

dressed ladder graphs (cf. fig. (4)) containing also vertex and self-energy corrections - an approach, pioneered by Gribov and Lipatov [5]. Integrating over a kinematic domain for intermediate gluons with ordered longitudinal momenta and strongly ordered transverse momenta, i.e.,

$$x < x_1 < x_2 < \ldots < x_n \; , \quad Q^2 \gg k_{T1}^2 \gg k_{T2}^2 \gg \ldots \gg k_{Tn}^2 \; , \quad (14)$$

one obtains the gluon density in the leading-logarithm approximation (LL(Q^2)A), which is identical to the result of the ordinary DGLAP evolution. In the case of strong ordering in longitudional and transverse momentum,

$$x \ll x_1 \ll x_2 \ll \ldots \ll x_n \; , \quad Q^2 \gg k_{T1}^2 \gg k_{T2}^2 \gg \ldots \gg k_{Tn}^2 \; , \quad (15)$$

one obtains the sum of all "double-logarithms" in Q^2 and $1/x$,

$$xg(x, Q^2) \sim \sum_n \frac{1}{n!^2} \left(\frac{12}{b_0} \ln \frac{\ln Q^2/\Lambda^2}{\ln Q_0^2/\Lambda^2} \ln \left(\frac{1}{x} \right) \right)^n \; . \quad (16)$$

This result is identical to eq. (13). Hence, the double-logarithm approximation (DLA) yields the QCD prediction for the gluon density at small x and sufficiently large Q^2.

One can also sum the ladder graphs in the case of strong ordering in x and no restriction on transverse momenta,

$$x \ll x_1 \ll x_2 \ll \ldots \ll x_n \; . \tag{17}$$

This yields the leading-logarithm approximation in $1/x$ (LL(1/x)A), which sums all powers $(\ln 1/x)^n$ for non-asymptotic values of Q^2. The derivative of the gluon density is obtained by the solution of the Balitsky-Fadin-Kuraev-Lipatov (BFKL) equation [15],

$$\frac{\partial}{\partial \ln 1/x} f(x,k_T^2) = \frac{3}{\pi}\alpha_s(M) k_\perp^2 \int_{k_0^2}^{\infty} \frac{dk_\perp'^2}{k_\perp'^2} \times \left[\frac{f(x,k_\perp'^2) - f(x,k_\perp^2)}{|k_\perp'^2 - k_\perp^2|} + \frac{f(x,k_\perp^2)}{(4k_\perp'^4 + k_\perp^4)^{1/2}} \right] , \tag{18}$$

where

$$f(x,Q^2) = Q^2 \frac{\partial}{\partial Q^2} x g(x,Q^2) \quad . \tag{19}$$

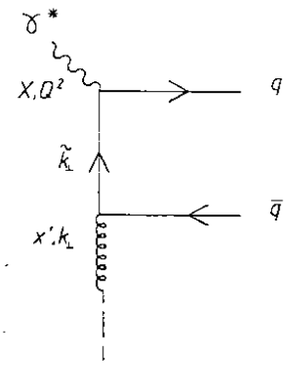

Figure 5: Pair production of light quarks in photon gluon fusion.

Here the scale of α_s is fixed and the integration starts at $k_0^2 = 0$. At small x the solution of the BFKL equation reads

$$\begin{aligned} x g(x,Q^2) &\sim x^{-\lambda} \; , \\ \lambda &= \frac{12\alpha_s}{\pi} \ln 2 \; . \end{aligned} \tag{20}$$

Choosing a reasonable scale for the fixed α_s, one obtains $\lambda \sim 0.5$. A comparison of eqs. (13) and (20) shows that the LL(1/x)A predicts an even more singular behaviour of the gluon density at small x than the DLA!

The predicted strong increase of the gluon density at small x is very interesting and appears to be in qualitative agreement with experimental data. There are, however, a number of important theoretical questions concerning this equation which remain to be answered. Probably the most important problem concerns the size of next-to-leading order corrections [16,17]. Other important issues are the relation to the double-logarithm approximation [18] and the dependence on the lower and the upper limit of integration [19-21].

Phenomenology of $F_2(x,Q^2)$ at low x

Askew, Kwiecinski, Martin and Sutton (AKMS) have used the BFKL equation to predict $F_2(x,Q^2)$ at small x [22]. Their starting point is the "$k_\perp$-factorization" [23] which is used to express the structure function in terms of the photon-gluon fusion cross section for quark pair production and the "unintegrated" gluon density $f(x,Q^2)$ [22](cf. fig. (5)),

$$F_2(x,Q^2) = \int_x^1 \frac{dx'}{x'} \int_{k_0^2}^{\infty} \frac{dk_\perp^2}{k_\perp^2} \times \hat{\sigma}_{\gamma g}\left(\frac{x}{x'}, k_\perp^2, Q^2\right) f(x',k_\perp^2) \; . \tag{21}$$

In the case of strong ordering this expression reduces to the result of the usual DGLAP evolution. Using as boundary condition in the BFKL equation (18) the gluon density $g(x_0 = 0.01, Q^2)$ determined from global fits, one obtaines a prediction for F_2 at values of x below 10^{-2}. The result, which is plotted in fig. (6), shows the experimentally observed strong increase at small x. However, the prediction is rather sensitive to the infrared cut-off k_0^2 in eq. (21). Less sensitive is the slope of the x-dependence, $\lambda = -\partial \ln \bar{F}_2 / \partial \ln x$, where $\bar{F}_2$ is the difference between F_2 and a "background" contribution to F_2, which is non-singular at small x [22].

In an alternative approach, Glück, Reya and Vogt (GRV) made a prediction for parton densities at low x by using the standard DGLAP evolution down to the very small input scale $Q_0^2 = 0.3\ \mathrm{GeV}^2$ [24]. At $Q^2 \gg Q_0^2$ and small x one then obtains the result of the double-logarithm approximation (13). For values of x around $\bar{x} = 10^{-3}$ and at $\bar{Q}^2 = 20\ \mathrm{GeV}^2$ one also has an effective power behaviour (cf. fig. (7)),

$$\begin{aligned} x g(x,Q^2) &\sim x^{-\lambda} \; , \\ \lambda &= \frac{1}{2}\left(\frac{48}{b_0} \ln \frac{\ln \frac{\bar{Q}^2}{\Lambda^2}}{\ln \frac{Q_0^2}{\Lambda^2}} \ln \frac{1}{\bar{x}} \right)^{1/2} \\ &= 0.47 \; . \end{aligned} \tag{22}$$

Hence, the AKMS prediction, based on the BFKL equation, and the GRV prediction, corresponding to the DLA with a non-singular input at a low momentum scale, are indistinguishable with present data. In principle, the BFKL and the DLA predictions can be distinguished by the different Q^2-dependence of the slope λ.

In both cases the growth of F_2 is a consequence of gluon radiation. This has to be contrasted with the Regge behaviour at small x. The successfull parametrization of the photon-proton total cross section by Donnachie and Landshoff [25] is based on the sum of Pomeron and Regge pole exchanges,

$$\sigma_{\gamma p} = \sum_{n=1}^{2} A_n s^{\alpha_n(0)-1} \quad . \tag{23}$$

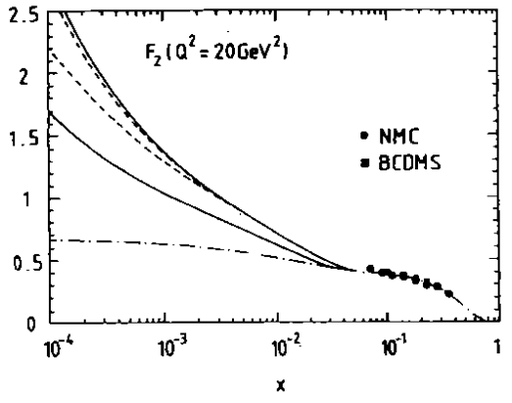

Figure 6: Prediction for the structure function $F_2(x, Q^2)$ at $Q^2 = 20$ GeV^2 based on the BFKL equation. For the three upper curves the infrared cut-off is chosen to be $k_0^2 = 1$ GeV^2, for the lower continuous curve it is $k_0^2 = 2$ GeV^2. For the dashed curves screening effects are included. From [22].

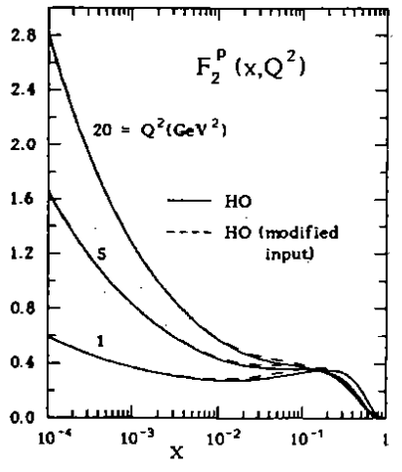

Figure 7: Prediction for the structure function $F_2(x, Q^2)$ at different values of Q^2 based on the DGLAP equation and "valence-like" input. From [24].

The corresponding prediction for the structure function at small x contains the same two Regge slopes,

$$F_2(x, Q^2) = \sum_{n=1}^{2} \tilde{A}_n(Q^2) \left(\frac{1}{x}\right)^{\alpha_n(0)-1} \quad , \tag{24}$$

where the phenomenological coefficient functions are chosen such that F_2 vanishes linearly as $Q^2 \to 0$, with Q^2/x fixed [26]. The corresponding prediction for F_2 is shown in fig. (8) for $Q^2 = 10$ GeV^2. It differs strongly from expectations based on perturbative QCD and appears to be disfavoured by present data [13,14].

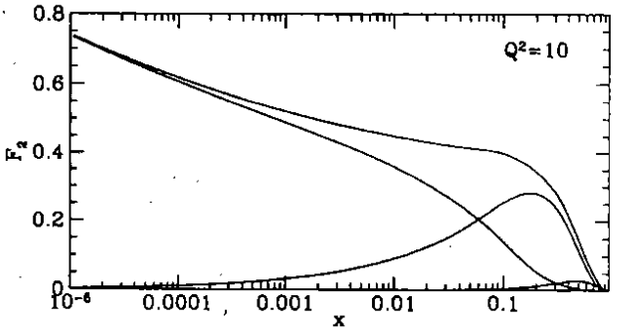

Figure 8: Prediction for the structure function $F_2(x, Q^2)$ at $Q^2 = 10$ GeV^2 based on Regge theory. The curves are the total, together with its valence, nonvalence and higher-twist components. From [26].

Screening Corrections at Low x

The growth of parton densities at small x predicted by perturbative QCD, either in the DLA or on the basis of the BFKL equation, violates asymptotically unitarity and is therefore unacceptable for $x \to 0$. One expects that the growth is tamed by "screening corrections", i.e., parton recombination processes of the type illustrated by the so-called "fan-diagram" fig. (9).

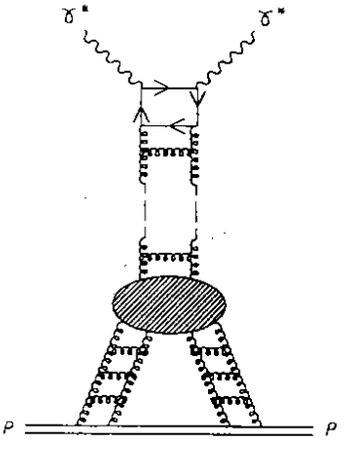

Figure 9: "Fan-diagram" contribution to screening corrections.

Such processes are taken into account by the nonlinear

Gribov-Levin-Ryskin (GLR) equation [27],

$$\frac{\partial}{\partial \ln \frac{1}{x}} xg(x,Q^2) = K \otimes f - \frac{81\alpha_s^2(Q^2)}{16Q^2R^2}\left(xg(x,Q^2)\right)^2 , \tag{25}$$

where K can be either the Altarelli-Parisi or the BFKL kernel. Note, that the GLR equation contains a dimensionful parameter, $1/R$, which in phenomenological applications is typically varied between 2 and 5 GeV. As a consequence, the GLR equation mixes contributions of all twists, in marked difference to the usual DGLAP evolution equation.

When do screening effects become important? According to a simple estimate [28] this is the case if the gluon density per unit of rapidity multiplied with the gluon "size" at the particular value of Q^2 is of order the proton size,

$$xg(x,Q^2)\pi r^2(Q) \sim \pi r_p^2 . \tag{26}$$

Here the gluon "size" $r(Q) \sim 2/Q$ and the proton size $r_p \sim 1$ fm. This yields

$$xg(x,Q^2) \sim 6\ Q^2[\mathrm{GeV}^2] , \tag{27}$$

which is 120 at $Q^2 = 20$ GeV^2. The set of parton densities D'_- of Martin et al. [9] predicts a gluon density of ~ 20 at $Q^2 = 20$ GeV^2 and $x = 5 \cdot 10^{-4}$. Hence, one may not anticipate strong screening effects in the HERA kinematic range.

Although qualitatively intriguing, the GLR equation does not provide a complete description of screening effects. The anomalous dimension of the four-gluon operator,

$$\gamma_{4,J} = 4\frac{\alpha_s}{J-1}(1+\delta^2) , \tag{28}$$

differs by a small amount $\mathcal{O}(\delta^2)$ from the prediction of the GLR equation [29,30], where $\delta^2 \approx 0.00955$ [30]. The anomalous dimension is not correctly reproduced by the GLR equation since interactions between the two lower gluon ladders in the fan-diagram fig. (9) are neglected. Although the change in the anomalous dimension is tiny, the interaction between the gluon ladders increases significantly the screening corrections as compared to the GLR equation [31].

Final States

In order to obtain a better understanding of the dynamics in the low-x region it will be crucial to investigate in detail final states in addition to structure functions. In principle, the BFKL growth of the gluon density at low x can be studied by observing particular, so-called "hot-spot" jets in the forward direction, which are characterized by the kinematic requirements $k_\perp^2 \sim Q^2$ and $x_B \ll x$ [28,32-35](cf. fig. (10)).

The differential cross section for the production of "hot-spot" jets shows the BFKL growth at small x_B,

$$\frac{d\sigma}{dx_B dQ^2 dx dk_\perp^2} \sim \tilde{f}(x,k_\perp^2)\left(\frac{x_B}{x}\right)^{-\lambda} . \tag{29}$$

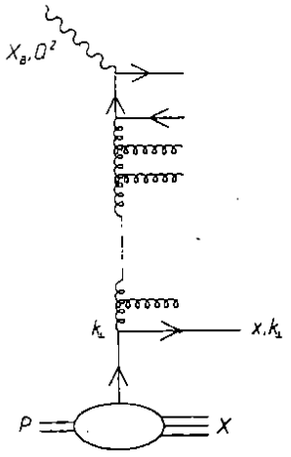

Figure 10: "hot-spot" jet diagram

Since $k_\perp^2 \sim Q^2$, the Q^2-evolution is separated from the x-dependence. This process could provide a clear signal for the BFKL growth. It is, however, experimentally demanding, and on the theoretical side one has to worry about non-perturbative corrections which become large for small values of $k_\perp^2$ [20].

Interesting "diffractive" events with large rapidity gaps have been reported at this conference by ZEUS and H1 [13,14]. Such events are not described by standard deep-inelastic Monte Carlo programs. However, they were not unexpected, and several mechanisms have been discussed in the literature [36-39]. One possibility is the exchange of a pomeron, as suggested by Ingelman and Schlein [36] (cf. fig. (11)).

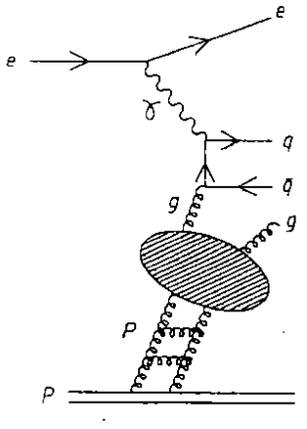

Figure 11: Pomeron contribution to diffractive process

Diffractive events at large Q^2 would then probe the structure function of the pomeron. ZEUS has also reported preliminary results on the contribution of these events to the structure function $F_2(x,Q^2)$ for different values of Q^2 [40]. This Q^2-dependence will be crucial for the interpretation of the diffractive events.

It is, of course, conceivable that also other, more unexpected phenomena will be discovered by studying final states in detail. An intriguing possibility is the instanton-induced, resonance-like production of minijet fireballs, as recently discussed by Balitsky and Braun [41].

Low-x Summary

The experimental observation of the rise of the structure function $F_2(x,Q^2)$ at small x is very interesting. The theoretical interpretation, however, is uncertain at present. So far, there is no theory which would allow a prediction together with an estimate of the error. Qualitatively, expectations based on perturbative QCD, exploiting either the DLA or the BFKL equation, are in agreement with data.

The growth predicted by both, DLA and BFKL, as $x \to 0$ cannot be correct since it is in conflict with unitarity. One expects, that DLA and BFKL are good approximations in certain x-intervals which depend on Q^2, i.e., $x_{min}(Q^2) < x < x_{max}(Q^2)$. Estimates for x_{min} range from 10^{-2} to 10^{-3} at $Q^2 = 16$ GeV^2 (cf. [1,15,42]).

On the experimental side, the study of specific final states, such as "hot-spot" jets and rapidity-gap events, will be crucial to unravel the dynamics at low x. On the theoretical side, the computation of next-to-leading order corrections in $\ln(1/x)$ is most important. Of course, a theoretical challenge is to understand the Regge limit, $x \to 0$, within QCD. Since the BFKL growth appears to be a phenomenon which is dominated by the gluon dynamics only, it may also be possible to gain some insight from lattice QCD in the quenched approximation.

Photoproduction

The dominant part of the ep cross section is in the photoproduction region, i.e., $Q^2 < 10^{-2}$ GeV^2. High-energy scattering between quasi-real photons and protons is of interest for a number of reasons [43,44], it allows in particular to study the hadronic structure of the photon by means of medium- to high-$p_\perp$ jets in the final state (cf. fig. (12)).

The physics of jets has been comprehensively reviewed by Catani at this conference [45]. Therefore, I shall only comment on one aspect where we can hope for some qualitative progress at HERA: the determination of the gluon densities in photon and proton. In general, for high-$p_\perp$ processes, photon-proton scattering is analogous to proton-proton scattering. The cross section is

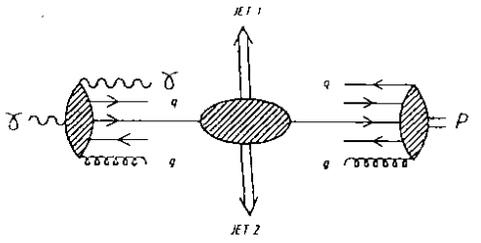

Figure 12: Photoproduction of two high-$p_\perp$ jets

obtained by an incoherent sum of parton-parton cross sections,

$$d\sigma_{\gamma p} = \sum_{a,b} \int dM \frac{dL_{ab}}{dM} d\hat{\sigma}_{ab}(M^2) \ , \qquad (30)$$

where the parton-parton luminosities are determined by the structure functions of proton and photon,

$$\frac{dL_{ab}}{dM} = \frac{2\tau}{M} \int_\tau^1 \frac{dx}{x} f_{a|\gamma}(x, M_\gamma) f_{b|p}(\frac{\tau}{x}, M_p) \ , \qquad (31)$$

with $\tau = M^2/s$. The quark and anti-quark content of the photon has already been measured in e^+e^- annihilation. A direct determination of the gluon content of the photon will be possible at HERA [46].

Recently, higher order QCD corrections [47] have been calculated for the resolved [48] and direct [49] contributions to one-jet and two-jet inclusive cross sections and also to inclusive particle production [50]. The gluon content of the photon is expected to be clearly visible in the $p_\perp$-spectrum below ~ 9 GeV and also in rapidity distributions. For inclusive hadron production the

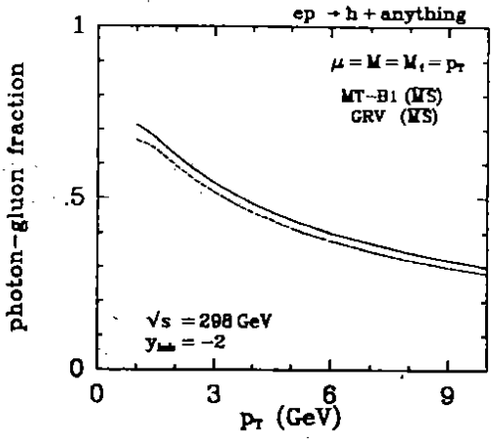

Figure 13: Fraction of the charged hadron production cross section due to gluon distribution in the photon. From [50].

theoretical prediction for the fraction of the production cross section due to $f_{g|\gamma} \neq 0$ is shown in fig. (13). Preliminary H1 data for the one-jet inclusive cross section already indicate the presence of a non-zero gluon component of the photon [51].

So far the evidence for the gluon density inside the proton is mostly indirect. At HERA a direct measurement will be possible in the range $10^{-3} < x < 10^{-1}$ using several techniques [52]. One method is based on open charm production [53]. The events are tagged by means

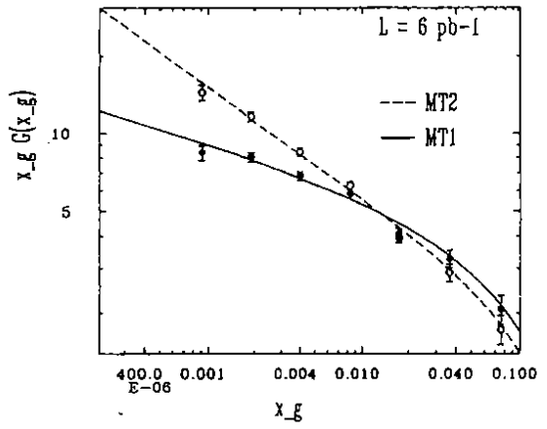

Figure 14: Reconstructed gluon densities from $D^{*\pm}$ production. From [53].

of D^*-mesons, and the momentum fraction x_g of the gluon is reconstructed using the Jacquet-Blondel method. The accuracy of the gluon density determination, which can be achieved with an integrated luminosity of 6 pb^{-1}, is apparent in fig. (14). Recently, also next-to-leading order QCD corrections have been calculated for the process of open charm production. It turns out that the background due to resolved photon processes can be suppressed by means of a cut on the invariant mass of the produced $c\bar{c}$ pair [54].

D-mesons

The total production cross section for $b\bar{b}$ and $c\bar{c}$ pairs is rather large. An integrated luminosity of 100 pb^{-1} will lead to $\sim 10^6$ $b\bar{b}$ and $\sim 10^8$ $c\bar{c}$ pairs, which yield $\sim 10^7$ D^0-mesons.

Using such a sample of charmed mesons one can significantly improve present limits on rare decays. One interesting example are leptonic decays (cf. [55])

$$D^0 \rightarrow \mu^+\mu^-, e^+e^-, \mu^\pm e^\mp \; . \qquad (32)$$

In the standard model the two, electron- and muon-number conserving processes are induced at one loop due to the mixing of quark flavours. The corresponding branching ratios are very small, of order 10^{-19}, and therefore unobservable for the forseeable future. However, in many extensions of the standard model branching ratios into two leptons are sizeable. Leptoquark exchange, for instance, can lead to branching ratios up to the present experimental upper bounds. In table (1) the current limits are compared with the limits obtainable at HERA. An improvement by about two orders of magnitude appears feasible [55].

Electroweak Processes

The two main electroweak processes are inelastic neutral current (NC) and charged current (CC) scattering. Of interest are also the production of charged and neutral intermediate vector bosons, and radiative charged current scattering. All these processes test certain aspects of the electroweak theory. From LEP we know that the standard model Higgs boson is heavier than about 60 GeV. The production cross section for Higgs bosons in this mass range in ep scattering is too small to be of relevance at HERA [56].

The inelastic scattering of left-handed and right-handed electrons off protons (cf. fig.(1)) is described by the differential cross section

$$\frac{d^2\sigma^{NC}}{dxdy}(e^-_{L,R}p) = \frac{2\pi\alpha^2}{x^2y^2s}\left[2(1-y)F_2^{L,R}(x,Q^2) + 2xy^2F_1^{L,R}(x,Q^2) + (1-(1-y)^2)xF_3^{L,R}(x,Q^2)\right] \; . (33)$$

Since the weak interactions violate parity, a third structure function F_3 appears together with F_1 and F_2.

In addition to the QCD scaling violations, the structure functions have a Q^2-dependence due to electroweak formfactors,

$$F_2^{L,R} = \sum_q x\left(q(x,Q^2) + \bar{q}(x,Q^2)\right) \times \left(|\, V_q^{L,R}(Q^2)\,|^2 + |\, A_q^{L,R}(Q^2)\,|^2\right) \; ,$$

	e^-e^-	$\mu^+\mu^-$	$e^\pm\mu^\mp$
current limits	$3 \cdot 10^{-5}$	$1 \cdot 10^{-5}$	$4 \cdot 10^{-5}$
HERA	$1 \cdot 10^{-7}$	$5 \cdot 10^{-7}$	$3 \cdot 10^{-7}$

Table 1: Branching ratios of D^0 into two leptons. From [55].

$$F_3^{L,R} = \pm \sum_q x \left(q(x,Q^2) - \bar{q}(x,Q^2)\right) \times V_q^{L,R}(Q^2) A_q^{L,R}(Q^2) . \quad (34)$$

The electroweak form factors $V_q^{L,R}(Q^2)$ and $A_q^{L,R}(Q^2)$ depend on the electric charges (Q_e, Q_q) and the vector (v_e, v_q) and axial-vector (a_e , a_q) couplings of electron and quarks to the Z-boson:

$$V_q^{L,R}(Q^2) = Q_e Q_q + (v_e \pm a_e) v_q \frac{Q^2}{Q^2 + m_Z^2} , \quad (35)$$

$$A_q^{L,R}(Q^2) = -(v_e \pm a_e) a_q \frac{Q^2}{Q^2 + m_Z^2} . \quad (36)$$

These form factors arise from the interference between photon and Z-boson exchange.

In the standard model of electroweak interactions vector and axial-vector couplings of electron and quarks can be expressed in terms of electric charge, weak isospin (T_3) and the weak angle θ_W, or, equivalently, in terms of the Fermi constant G_μ, the Z-boson mass m_Z and the fine-structure constant α ($f = e, q$):

$$v_f = \frac{1}{\sin 2\theta_W} \left(T_3^f - 2Q_f \sin {\theta_W}^2\right) , \quad (37)$$

$$a_f = \frac{1}{\sin 2\theta_W} T_3^f , \quad (38)$$

where

$$\sin^2 \theta_W = 1 - \frac{m_W^2}{m_Z} , \quad (39)$$

$$\frac{1}{\sin 2\theta_W} = \frac{1}{2} \left(\frac{\sqrt{2} G_\mu m_Z^2}{\pi \alpha} \right)^{1/2} . \quad (40)$$

The relation between the weak angle and the vector boson masses holds at tree-level. If radiative corrections are included this is one possible definition of the weak angle.

In addition to neutral current processes charged current reactions are of importance at HERA. The order of magnitude of the total charged current cross section is $\sigma_{tot}^{CC} \sim G_F^2 s/4\pi \sim 100$ pb at the HERA c.m.s energy, yielding $\sim 10^4$ charged current events for an integrated luminosity of 100 pb^{-1}.

Precision Tests

Higher order electroweak corrections to neutral current scattering involve electromagnetic bremsstrahlung and electroweak virtual corrections. A complete evaluation of the one-loop corrections has been performed independently by two groups [57]. The bremsstrahlung contribution has to be integrated over the region of phase space where the additional photon cannot be observed. This yields particularly large corrections at small values of x and Q^2. However, for electroweak precision tests the region $Q^2 > 10^3$ GeV^2 is important, and here the bremsstrahlung contribution is rather small.

In order to discuss next-to-leading order electroweak corrections one has to specify first of all a renormalization scheme. Convenient and transparent with respect to its physical meaning is the on-shell scheme where the electromagnetic fine-structure constant α and the masses of W-boson (m_W), Z-boson (m_Z), Higgs-boson (m_H) and top-quark (m_t) appear as independent parameters. The Fermi constant, as measured in μ-decay, is then a dependent quantity,

$$G_\mu = G_\mu(\alpha, m_W, m_Z, m_H, m_t) . \quad (41)$$

Since the Fermi constant is known to high precision it is often convenient to use instead a modified on-shell scheme where G_μ replaces m_W as independent variable.

The sum of the Born-amplitude and the one-loop corrections can be expressed as sum of a dressed photon-exchange amplitude and a dressed Z-boson exchange amplitude. The structure of the dressed amplitudes [58] is similar to the Born amplitudes, the main difference is the appearance of a variety of form factors. From eqs. (35)-(40) it is clear that the strength of the Z-exchange amplitudes is proportional to $G_\mu m_Z^2$. The one-loop corrections lead to a formfactor [58]

$$G_\mu m_Z^2 \rightarrow G_\mu m_Z^2 \rho_{eq}(x,Q^2) , \quad (42)$$

where

$$\rho_{eq}(x,Q^2) = 1 + \Delta\rho + \Delta_{eq}(x,Q^2) . \quad (43)$$

Here

$$\Delta\rho = \frac{3\alpha}{4\pi \sin^2 2\theta_W} \frac{m_t^2}{m_Z^2} \quad (44)$$

is a universal part and Δ_{eq} is an additional non-universal correction. Similarly, the mixing angle which appears in the vector coupling v_f (cf. (37)) now becomes a form factor which depends on the quark species [58]

$$\sin\theta_W \rightarrow s_{eq}(x,Q^2) , \quad (45)$$

where

$$s_{eq}^2(x,Q^2) = \sin^2\theta_W (1 + \cot^2\theta_W \Delta\rho + \Delta_q(x,Q^2)) . \quad (46)$$

Δ_q is again a non-universal contribution. In addition to the formfactors which affect normalization and $Z-\gamma$ - mixing there are also some non-factorizable terms [58]. The magnitude of the one-loop corrections to the Born amplitudes is of order 1%.

What can we learn from precision measurements at HERA for the theory of electroweak interactions? A

particularly useful quantity is the ratio

$$R_- = \frac{d\sigma^{NC}(x,Q^2)}{d\sigma^{CC}(x,Q^2)} , \qquad (47)$$

integrated over some optimized range in x and Q^2. According to the analysis of Brisson et al. [59] a measurement of R_- with 1% accuracy appears ultimately feasible at HERA. For each Higgs mass this measurement defines a thin band in the m_W-m_t-plane. For two Higgs masses these bands are shown in fig. (15). Also shown are the corresponding lines which result from the G_μ constraint. There is a difference in curvature due to the propagator effect. Clearly, the measurement of R_- is effectively a determination of the Fermi "constant"

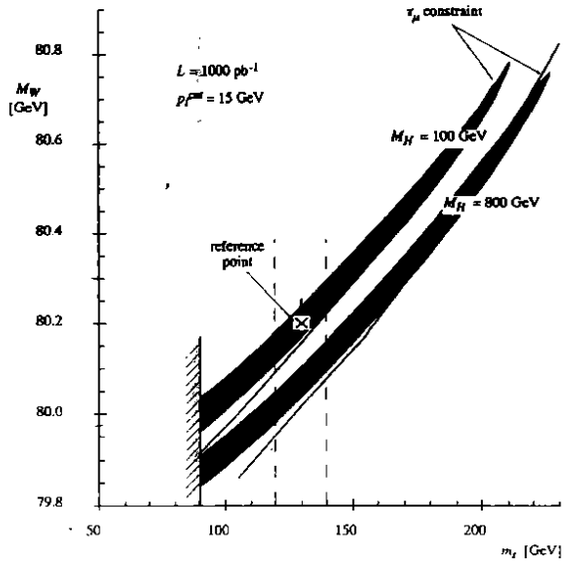

Figure 15: 1σ-contours obtained from a measurement of R_- for two values of the Higgs mass. The two lines are the corresponding constraints from the muon lifetime. From [59].

at large values of Q^2, whereas muon decay yields a determination at $Q^2 = 0$. Both measurements restrict the W-boson mass with comparable accuracy. For instance, let us assume that the top-quark mass is known with an error of 10 GeV and that the central value is 130 GeV (a result with such a precision may eventually be obtained by the Tevatron experiments). One then reads off from fig. (15) that the R_- measurement restricts the W-mass with an error of

$$\delta m_W = \pm\, 160\,\mathrm{MeV} \quad . \qquad (48)$$

It is a non-trivial test of the electroweak theory that the Fermi "constants" at small and large values of Q^2 yield consistent values of m_W. A further crucial test of the standard model, and a restriction on physics beyond the standard model, is the consistency between the W-boson masses determined from the propagator and from W-pair production at LEPII.

Production of Vector Bosons

In inelastic electron-proton collisions photons, W-bosons and Z-bosons can be produced. There are two types of processes,

$$\begin{aligned} e^- p &\rightarrow e^- (\gamma, Z, W^\pm) X \quad , \\ e^- p &\rightarrow \nu (\gamma, Z, W^-) X \quad . \end{aligned} \qquad (49)$$

In recent years detailed calculations for vector boson production in ep-collisions have been carried out [60]. For the total production cross section one finds [60]

$$\sigma^{tot}(ep \rightarrow WX) \sim 3\, \sigma^{tot}(ep \rightarrow ZX) \sim 1\mathrm{pb} \, . \qquad (50)$$

Particularly interesting are the clean diffractive processes $e^- p \rightarrow \nu W^- p$, $e^- p \rightarrow e^- Z p$, whose cross sections are about 1/3 of the corresponding inelastic cross sections [60].

The production of vector bosons at HERA can be used to test the standard model predictions for the couplings of W-bosons to photons. In extensions of the standard model "anomalous" couplings can occur. The corresponding parameters κ and λ are related to the magnetic dipole moment and the electric quadrupole moment of the W-boson. The limits on anomalous gauge couplings obtainable at HERA appear to be weaker than the bounds which can be expected from the Tevatron and LEPII within the next few years [61].

Contact Interactions

Low energy effects of new interactions can be systematically studied by means of non-renormalizable, effective lagrangians. For neutral current processes the most general lagrangian reads [62,63],

$$\mathcal{L}^{eN}_{contact} = \mathcal{L}^{eN}_V + \mathcal{L}^{eN}_S \, , \qquad (51)$$

where the chirality conserving part reads

$$\begin{aligned} \mathcal{L}^{eN}_V = \sum_{q=u,d} & [\eta^q_{LL}(\bar{e}_L\gamma_\mu e_L)(\bar{q}_L\gamma^\mu q_L) \\ & +\eta^q_{LR}(\bar{e}_L\gamma_\mu e_L)(\bar{q}_R\gamma^\mu q_R) \\ & +\eta^q_{RL}(\bar{e}_R\gamma_\mu e_R)(\bar{q}_L\gamma^\mu q_L) \\ & +\eta^q_{RR}(\bar{e}_R\gamma_\mu e_R)(\bar{q}_R\gamma^\mu q_R)] \quad , \end{aligned} \qquad (52)$$

and the chirality changing part is

$$\begin{aligned} \mathcal{L}^{eN}_S = & \eta_d(\bar{e}_L e_R)(\bar{d}_R d_L) + \eta_u(\bar{e}_L e_R)(\bar{u}_L u_R) \\ & +\tilde{\eta}_u(\bar{e}_L u_R)(\bar{u}_L e_R) \, . \end{aligned} \qquad (53)$$

Here we have assumed an underlying $SU(2)_L \times U(1)_Y$, thus only three of the possible six chirality flip terms appear. Furthermore, among the chirality conserving contact terms one has the relation $\eta^u_{RL} = \eta^d_{RL}$.

Contact interactions can be generated by the exchange of heavy intermediate particles. Examples are leptoquarks and heavy neutral Z'-vector bosons. Different exchange particles lead to different sets of non-vanishing η-coefficients. Therefore it is important to disentangle the various different contact terms in order to identify the underlying physics.

Adding contact interactions to the standard model lagrangian, an observed deviation from the standard model prediction for the neutral current cross section can be related to a size of any single η-coefficient which is assumed to be non-zero. Recently, a detailed combined analysis for all 8 η-parameters of the chirality conserving contact terms has been performed [64]. The sensitivity depends on the integrated luminosity and on the polarization of the incident electron or positron. In the general analysis one considers all 28 projections in the 8-dimensional η-space.

The study of contact interactions is not very relevant for weakly coupled new particles. In this case the obtained mass bounds are so low that the particle under consideration can usually be directly produced. Interesting mass bounds are obtained for strongly coupled particles. Here one can probe mass scales up to $(\eta \equiv 4\pi/\Lambda^2)$

$$\Lambda \approx 7 TeV \ , \tag{54}$$

which may be further improved if charged current contact terms, related by $SU(2)_L$-invariance, are taken into account [65]. Note, however, that electron-quark contact interactions are already strongly constrained from low energy precision experiments, in particular from atomic parity violation [66].

New Particles

The structure of the standard model of strong and electroweak interactions poses to a number of questions which lead us beyond the standard model. Do elementary scalar particles exist? Is lepton number an exact or an approximate symmetry? Are the mass scales of electroweak symmetry breaking and supersymmetry breaking the same? All these questions motivate the search for new elementary particles.

Supersymmetry

Let us first discuss the prospects for producing super-particles at HERA. The super-particle mass spectrum is largely arbitrary. However, several calculations have recently been performed where the unification of the gauge couplings, the idea of radiative electroweak symmetry breaking and some constraints concerning fine-tuning of parameters have been implemented [67]. In a large class of models the masses of photino ($\tilde{\gamma}$), zino ($\tilde{z}$), winos ($\tilde{w}$), scalar leptons ($\tilde{l}$), scalar quarks ($\tilde{q}$) and gluino ($\tilde{g}$) satisfy the inequalities

$$m_{\tilde{\gamma}}, m_{\tilde{z}}, m_{\tilde{w}} < m_{\tilde{l}} < m_{\tilde{q}} < m_{\tilde{g}} \ , \tag{55}$$

where the electroweak gaugino masses are of order 100 GeV, the masses of scalar leptons are of order 200 GeV, and scalar quark masses vary from 350 GeV to 600 GeV.

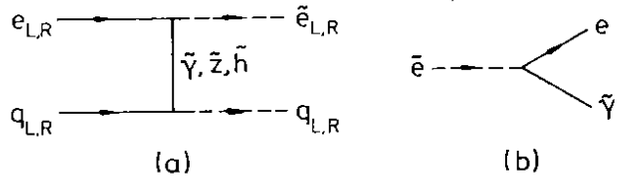

Figure 16: (a) Pair production of scalar electrons and scalar quarks; (b) scalar electron decay.

At HERA the most obvious production process for super-particles is [68] (cf. fig. (16))

$$e\,p \rightarrow \tilde{e}\,\tilde{q}\,X. \tag{56}$$

The total cross section falls below 0.05 pb for $m_{\tilde{e}} + m_{\tilde{q}} > 200$ GeV [69]. Hence, in view of the present mass bounds for scalar leptons and scalar quarks from LEP and the Tevatron, this process will very likely not be of relevance at HERA.

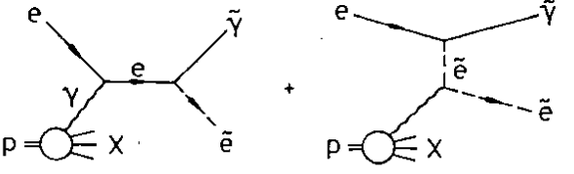

Figure 17: Production of scalar electron and photino

For light photinos a very interesting process is [70] (cf. fig. (17))

$$e\,p \rightarrow \tilde{e}\,\tilde{\gamma}\,X. \tag{57}$$

It is a Compton-type process with a bremsstrahlung photon radiated by the proton. This process is of higher order in the coupling than the previous one, but for $m_{\tilde{\gamma}} = 20$ GeV and $m_{\tilde{e}} = 60$ GeV the cross section is still about 0.05 pb [69]. This process could be seen at HERA, extending somewhat the reach for supersymmetry at LEPI.

A few years ago, Drees and Zeppenfeld [71] pointed out that the cross section for elastic production of scalar

electrons and photinos is as large as the inelastic cross section, i.e., $\sigma(ep \rightarrow \tilde{e}\tilde{\gamma}p) \approx \sigma(ep \rightarrow \tilde{e}\tilde{\gamma}X)$. The elastic process is interesting, especially since it leads to a very clean final state. The total cross section [72] for the inelastic, the elastic and the quasi-elastic processes are shown in fig. (18). Note, that in future high-energy ep colliders one may also be able to search for supersymmetry by using Compton back-scattered laser light. For an electron-proton c.m.s energy of 1 TeV the cross section for the production of wino pairs exceeds 1 fb for $m_{\tilde{w}} < 190$ GeV [73].

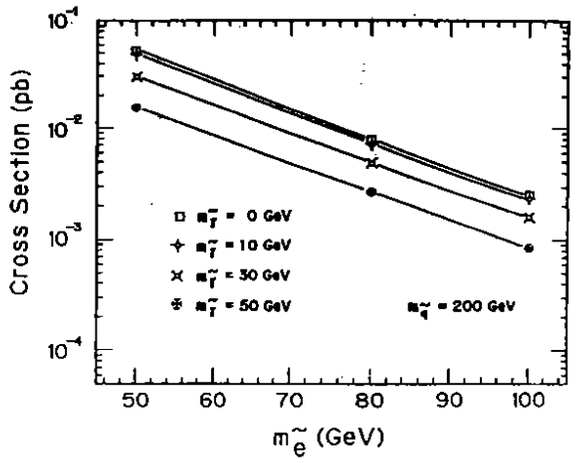

Figure 18: Total cross section for $ep \rightarrow \tilde{e}\tilde{\gamma}X$. From [72].

Leptoquarks

The theoretical framework for leptoquarks with Yukawa couplings to quark-lepton pairs are extended gauge theories. It is remarkable that such scalar particles with masses of order 100 GeV can be consistent with all constraints from rare processes, which have recently been discussed in great detail [74,75]. However, one should be aware of the fact that for most leptoquarks some fine tuning of couplings is required and that the most general couplings to quark-lepton pairs are usually not compatible with constraints from low energy data. In composite models and technicolour theories leptoquarks appear as pseudo-Goldstone bosons, which have derivative couplings to fermions pairs.

Leptoquarks with dimensionless couplings to fermion pairs must have spin 0 or spin 1. If, by convention, they all carry lepton number +1, their baryon number can be $+\frac{1}{3}$ or $-\frac{1}{3}$. The couplings of all possible leptoquarks to quark-lepton pairs have been classified in [76]. A particularly well studied example is the SU(5)-type leptoquark S_0 whose coupling to SU(2)-doublets is given by

$$\mathcal{L}_I = \lambda_L \, \bar{q}_L^c i\tau_2 l_L S_0^\dagger + c.c. \, . \qquad (58)$$

The couplings of scalar leptoquarks are of Yukawa type, and therefore their size may be similar to the size of Higgs boson couplings. In ordinary grand unified theories leptoquark masses are of order 10^{10} GeV or larger. However, in theories where Yukawa couplings violate the unified symmetry, leptoquarks may have masses of order m_W. In this case baryon- and lepton-number are conserved in the low-energy effective theory.

At HERA leptoquarks can be produced as s-channel resonances in the electron-quark subprocess shown in fig. (19).

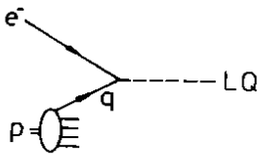

Figure 19: Leptoquark production in electron-quark annihilation

Since their width is small they appear as narrow resonances in the x-distributions of neutral and charged current cross sections. For a leptoquark mass $m_{LQ} \sim 200$ GeV and a coupling $\alpha_{LQ} \equiv \lambda_L^2/4\pi = \alpha_{em}$ the production cross is $\sigma_{LQ} \sim 10^2$ pb. Because of this rather large cross section HERA is well suited to search for leptoquarks. For $\alpha_{LQ} \sim \alpha_{em}$, leptoquarks can be discovered up to the kinematic limit, i.e., $m_{LQ} \sim 300$ GeV, and for the small coupling $\alpha_{LQ} \sim 10^{-3}\alpha_{em}$ one can still find leptoquarks up to $m_{LQ} \sim 200$ GeV. Discovery limits for all leptoquarks have been determined by means of detailed Monte Carlo studies [77].

First bounds on leptoquark masses have been reported at this conference by the collaborations H1 and ZEUS based on an integrated luminosity of 25 nb^{-1}. For left-handed couplings and $\alpha_{LQ} = \alpha_{em}$ both collaborations find lower bounds on leptoquark masses of about 170 GeV [13,14].

In supersymmetric models with broken R-parity single production of super-particles is possible. In these models scalar quarks can have direct couplings to electron-quark pairs. Hence, they can be produced in ep scattering like leptoquarks and similar bounds on their masses can be expected from HERA experiments [78].

Heavy Neutrinos

In extended gauge theories lepton number corresponds to a spontaneously broken local symmetry. A priori the scale of this symmetry breaking can be anywhere between the Fermi scale of weak interactions and the grand unification scale $\Lambda_{GUT} \sim 10^{16}$ GeV. A large

scale of B-L breaking implies very small neutrino masses, which may be in the range needed to explain the solar neutrino deficit by means of the MSW-mechanism. In this case we expect no neutral heavy leptons and also no new vector bosons, such as a Z', at energies accessible with accelerators.

Alternatively, some theories predict a low scale of B-L breaking, $\Lambda_{B-L} = \mathcal{O}(1\,\mathrm{TeV})$. In this case, the ordinary neutrinos are expected to have masses close to the present experimental upper limits. Furthermore, additional vector bosons (W_R and/or Z') and new heavy neutrinos with masses in the range from a few tens of GeV to a few hundred GeV are predicted. Low energy processes and LEP data require the W_R-boson to be heavier than 450 GeV [79]. The lower bound increases to 520 GeV, if the lightest right-handed neutrino has a mass below 15 GeV [80]. This leaves an interesting range of ν_R and W_R masses which can be probed for the first time at HERA. In left-right symmetric models with spontaneous parity breaking W_R-bosons have to be heavier than 1 - 3 TeV [81]. This mass range lies beyond the sensitivity of HERA.

Heavy neutrinos are the simplest example of new heavy leptons and quarks which can be produced via mixing in charged and neutral current processes in ep scattering (cf. fig. (20)). In the literature new heavy fermions have been discussed in connection with E_6 unified theories, a fourth generation and mirror families [82].

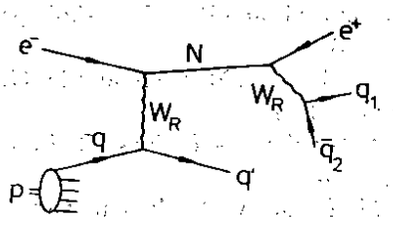

Figure 20: Production and decay of heavy Majorana neutrinos via W_R exchange.

The production of heavy neutrinos can proceed in several ways, depending on the model. A striking signature is the possible change of lepton number by two units due to the Majorana nature of the heavy neutrinos (cf. fig. (20)). In left-right symmetric models the dominant process is W_R exchange, whereas in Z' models the mass mixing between light and heavy neutrinos leads to production in ordinary charged current reactions. Constraints from low energy experiments on elements of the mixing matrix ξ_{ij} typically yield $|\,\xi\,| < 0.1$ [83]. For an integrated luminosity of 200 pb^{-1}, a rough estimate of the discovery limits for heavy neutrinos and W_R-boson in left-right symmetric models yields a maximal neutrino mass of 120 GeV and a maximal vector boson mass of about 700 GeV. In Z' models, for a maximal mixing parameter $|\,\xi\,| = 0.1$, the discovery limit for heavy neutrinos is 160 GeV. Detailed Monte Carlo studies, including background processes, have been carried out by several groups [84].

A comprehensive study of other heavy leptons which could be produced at HERA has been performed in [85]. For charged heavy leptons, which couple to electrons via mixing in the neutral current, the production cross section is slightly smaller than for heavy neutrinos. In composite models heavy states can couple to ordinary leptons and vector bosons via non-renormalizable derivative couplings. For a compositeness scale of 1 TeV one is sensitive to excited electrons and neutrinos with masses up to about 200 GeV and 150 GeV, respectively.

A low scale of B-L breaking, $\Lambda_{B-L} = \mathcal{O}(1\,\mathrm{TeV})$, predicts new particles, heavy vector bosons and new heavy leptons, which could be produced at present and future colliders. However, from a cosmological point of view this possibility appears to be disfavoured. The need to explain the cosmological baryon asymmetry imposes stringent constraints on the masses of the new states. They have to be much heavier than the W-boson unless the baryon asymmetry can be generated at the electroweak phase transition [86].

Summary

In the past deep-inelastic lepton-nucleon scattering has played a crucial role in testing QCD. In recent years detailed next-to-leading order analyses have been carried out for fixed target experiments, and the strong coupling constant has been determined with an accuracy of about 5%.

At higher energies lepton-nucleon scattering will continue to probe QCD. At HERA the region of small x below $\sim 10^{-3}$ and large $Q^2 \geq 10$ GeV^2 can be explored for the first time. This will improve our understanding of the interface between perturbative and non-perturbative QCD. The observed increase of the structure function F_2 suggests that the ideas of perturbative QCD are still applicable in this kinematic domain, although unequivocal theoretical predictions are still lacking. Another important topic will be the measurement of the gluon densities in proton and photon over a wide range in x.

HERA is also a charm factory. An integrated luminosity of 100 pb^{-1} will yield $\sim 10^8$ $c\bar{c}$ pairs. This will lead to a considerable improvement of present limits on rare D-meson decays, in the case of leptonic decays by two orders of magnitude.

With respect to electroweak processes the measurement of the strength of the charged current at $Q^2 \approx 10^4$ GeV^2 appears to be most interesting. Within the standard model, after the discovery of the top-quark, one expects to reach an accuracy for the W-boson mass of $\delta m_W = \pm 160$ MeV. This is comparable to the present constraint obtained from the Fermi constant at $Q^2 = 0$.

A model independent window to new physics are contact interactions. For chirality conserving and chirality changing neutral current contact terms HERA experiments can probe mass scales up to $\Lambda \sim 7$ TeV.

In the search for supersymmetry HERA can somewhat extend the reach of LEPI with respect to scalar electrons and photinos. Furthermore, models with broken R-parity can be tested. In this case single production of scalar quarks is possible. This is similar to leptoquark production for which HERA is an ideal collider. Even for the small coupling $\alpha_{LQ} \sim 10^{-3}\alpha_{em}$, for instance, leptoquarks with masses up to $m_{LQ} \sim 200$ GeV could be discovered. Also interesting is the single production of charged and neutral heavy leptons where, depending on the model, masses up to ~ 150 GeV can be reached.

Acknowledgements

I am grateful to my colleagues at DESY and to many participants of the Marseille conference for their help during the preparation of this report. Special thanks are due to J. Bartels for sharing his insight into low-x QCD.

References

[1] D. J. Gross, in *Methods in Field Theory*, Les Houches 1975, eds. R. Balin and J. Zinn-Justin (North-Holland, Amsterdam) p. 142.
[2] F. J. Yndurain, *Quantum Chromodynamics* (Springer-Verlag, 1983).
[3] G. Altarelli and G. Parisi, *Nucl. Phys.* **B126** (1977) 298.
[4] Yu. L. Dokshitzer, *JETP* **46** (1977) 641.
[5] V. N. Gribov and L. N. Lipatov, Sov. J. Nucl. Phys. **15** (1972) 78.
[6] R. G. Roberts, *these proceedings.*
[7] CTEQ collaboration: J. Botts et al., *Phys. Lett.* **304B** (1993) 159.
[8] M. Glück, E. Reya and A. Vogt, *Z. Phys.* **C48** (1990) 471; *Z. Phys.* **C53** (1992) 127; *Phys. Lett.* **306B** 391.
[9] A. D. Martin, W. J. Stirling and R. G. Roberts, *Phys. Rev.* **D47** (1993) 867; *Phys. Lett.* 306B (1993) 145.
[10] M. Klein, **HERA92**†, p. 71.
[11] Zeus collaboration: S. Bentvelsen, *these proceedings.*
[12] J. Blümlein and M. Klein, **HERA92**, p. 101.
[13] H1 collaboration: A. De Roeck, *these proceedings.*
[14] ZEUS collaboration: R. Klanner, *these proceedings.*
[15] E. A. Kuraev, L. N. Lipatov and V. S. Fadin, *Sov. Phys. JETP* **44** (1976) 443; **45** (1977) 199;
Ya. Ya. Balitskii and L. N. Lipatov, *Sov. J. Nucl. Phys.* **28** (1978) 822.
[16] V. Fadin and L. N. Lipatov, preprint DTP/93/08 (1993).
[17] J. Bartels, *Z. Phys.* **C60** (1993) 471.
[18] S. Catani et al., *Nucl. Phys.* **B336** (1990) 18; *ibid.* **B361** (1991) 645; G. Marchesini and B. R. Webber, *Nucl. Phys.* **B349** (1991) 617.
[19] J. C. Collins and P. V. Landshoff, *Phys. Lett.* **276B** (1992) 196.
[20] J. Bartels and H. Lotter, *Phys. Lett.* **309B** (1993) 400.
[21] J. Forshaw, P. Harriman and P. J. Sutton, preprint RAL-93-039 (1993).
[22] A. J. Askew, J. Kwiecinski, A. D. Martin and P. J. Sutton, *Phys. Rev.* **D47** (1993) 3775;
preprint DTP/93/38 (1993).
[23] S. Catani, M. Ciafaloni and F. Hautmann, *Phys. Lett.* **242B** (1990) 91; *Nucl. Phys.* **B336** (1991) 135.
[24] M. Glück, E. Reya and A. Vogt, *Phys. Lett.* **306B** (1993) 391.
[25] A. Donnachie and P. V. Landshoff, *Phys. Lett.* **B296** (1992) 227.
[26] A. Donnachie and P. V. Landshoff, preprint DAMTP 93-23 (1993).
[27] L. V. Gribov, E. M. Levin and M. G. Ryskin, *Phys. Rep.***100** (1983) 1.
[28] A. H. Mueller, *Nucl. Phys.* **B** (Proc. Suppl.) **18C** (1990) p. 125.
[29] E. M. Levin, M. G. Ryskin and A. G. Shuvaev, *Nucl. Phys.* **B387** (1992) 589.
[30] J. Bartels, *Phys. Lett.* **298B** (1993) 204.
[31] J. Bartels and M. G. Ryskin, *Z. Phys.* **C60** (1993) 751.
[32] J. Bartels, A. de Roeck and M. Loewe, *Z. Phys.* **C54** (1992) 635.
[33] W. K. Tang, *Phys. Lett.* **278B** (1992) 363.
[34] J. Kwiecinski, A. D. Martin and P. J. Sutton, *Phys. Lett.* **B287** (1992) 254; *Phys. Rev.* **D46** (1992) 921.
[35] E. Laenen and E. Levin, *J. Phys.* **G19** (1993) 1582.
[36] G. Ingelman and P. Schlein, *Phys. Lett.* **152B** (1985) 256.
[37] A. Donnachie and P. V. Landshoff, *Phys. Lett.* **B191** (1987) 309.
[38] N. N. Nikolaev and B. G. Zakharov, *Z. Phys.* **C49**

†Proc. of the Workshop *Physics at HERA*, eds. W. Buchmüller and G. Ingelman (Hamburg, 1992)

(1991) 607.
[39] K. H. Streng, *Proc. of the HERA Workshop*, ed. R. D. Peccei (Hamburg, 1988) p. 365;
M. G. Ryskin and M. Besancon, **HERA92**, p. 217.
[40] ZEUS collaboration: I. Park, *these proceedings.*
[41] I. I. Balitsky and V. M. Braun, preprint MPI-Ph/93-17 (1993).
[42] M. G. Ryskin, *Sov. J. Nucl. Phys.* **47** (1988) 230.
[43] G. A. Schuler, **HERA92**, p. 461.
[44] A. Levy, **HERA92**, p. 481.
[45] S. Catani, *these proceedings.*
[46] M. Drees and R. M. Godbole, *Phys. Rev.* **D39** (1989) 169.
[47] D. Bödeker, *these proceedings.*
[48] L. E. Gordon and J. K. Storrow, *Phys. Lett.* **291B** (1992) 320;
G. Kramer and S. G. Salesch, *Phys. Lett.* **317B** (1993) 218; preprint DESY 93-010 (1993);
M. Greco and A. Vicini, preprint LNF-93/017-P (1993).
[49] D. Bödeker, *Phys. Lett.* **292B** (1992) 164; *Z. Phys.* **C59** (1993) 501.
[50] F. M. Borzumati, B. A. Kniehl and G. Kramer, *Z. Phys.* **C59** (1993) 341.
[51] A. Rostovtsev, *these proceedings.*
[52] A. Ali and D. Wyler, **HERA92**, p. 669.
[53] R. van Woudenberg et al., **HERA92**, p. 739.
[54] S. Frixione et al., *Phys. Lett.* **308B** (1993) 137.
[55] S. Egli et al., **HERA92**, p. 770.
[56] K. J. F. Gaemers, R. M. Godbole and M. van der Horst, in *Proc. of the HERA Workshop*, ed. R. D. Peccei (Hamburg, 1988) p. 739.
[57] M. Böhm and H. Spiesberger, *Nucl. Phys.* **B294** (1987) 1081; *ibid.* **B304** (1988) 749; H. Spiesberger, *ibid.* **B349** (1991) 109;
D. Bardin et al., *Z. Phys.* **C42** (1989) 679; *ibid.* **C44** (1989) 149.
[58] W. Hollik et al., **HERA92**, p. 923.
[59] V. Brisson et al., **HERA92**, p. 947.
[60] U. Baur, J. A. M. Vermaseren and D. Zeppenfeld, *Nucl. Phys.* **B375** (1992) 3.
[61] U. Baur and M. Doncheski, *Phys. Rev.* **D46** (1992) 1959.
[62] R. Rückl, *Phys. Lett.* **129B** (1983) 363; *Nucl. Phys.* **B234** (1984) 91.
[63] W. Buchmüller, B. Lampe and N. Vlachos, *Phys. Lett.* **197B** (1987) 379.
[64] P. Haberl, F. Schrempp and H.-U. Martyn, **HERA92**, p. 1133.
[65] M. A. Doncheski and J. L. Hewett, *Z. Phys.* **C56** (1992) 209.
[66] P. Langacker, *Phys. Lett.* **256B** (1991) 277.
[67] G. G. Ross and R. G. Roberts, *Nucl. Phys.* **B377** (1992) 571;
R. Arnowitt and P. Nath, *Phys. Rev. Lett.* **69** (1992) 725;
S. Kelley et al., *Nucl. Phys.* **B398** (1993) 3.
[68] S. K. Jones and C. H. Llewellyn Smith, *Nucl. Phys.* **B217** (1983) 145.
[69] A. Bartl et al., **HERA92**, p. 1118.
[70] G. Altarelli et al., *Nucl. Phys.* **B262** (1985) 204.
[71] M. Drees and D. Zeppenfeld, *Phys. Rev.* **D39** (1989) 2536.
[72] H. Tsutsui et al., *Phys. Lett.* **245B** (1990) 663.
[73] W. Buchmüller and Z. Fodor, *Phys. Lett.* **316B** (1993) 510.
[74] M. Leurer, preprint WIS-93/90/Sept-PH (1993).
[75] S. Davidson, D. Bailey and B. A. Campbell, preprint CFPA-93-TH-29 (1993).
[76] W. Buchmüller, R. Rückl and D. Wyler, *Phys. Lett.* **B191** (1987) 442.
[77] P. Schleper, **HERA92**, p. 1043;
B. Andrieu et al., **HERA92**, p. 1059.
[78] J. Butterworth and H. Dreiner, **HERA92**, p. 1079;
T. Kon, T. Kobayashi and K. Nakamura, **HERA92**, p.1088.
[79] J. Polak and M. Zralek, *Nucl. Phys.* **B363** (1991) 385; *Phys. Lett.* **B276** (1992) 492;
W. Buchmüller and C. Greub, *Nucl. Phys.* **B381** (1992) 109.
[80] F. Abe et al., *Phys. Rev. Lett.* **67** (1991) 2609.
[81] G. Beall, M. Bender and A. Soni, *Phys. Rev. Lett.* **48** (1982) 848;
G. Ecker and W. Grimus, *Nucl. Phys.* **B258** (1985) 328.
[82] F. M. L. Almeida Jr., J. A. Martins Simões, A. J. Ramalho, *Nucl. Phys.* **B347** (1990) 537;
F. Csikor and I. Montvay, *Phys. Lett.* **231B** (1989) 503; F. Csikor, *Z. Phys.* **C49** (1991) 129.
[83] P. Langacker and D. London, *Phys. Rev.* **D38** (1988) 907;
W. Buchmüller, C. Greub and H.-G. Kohrs, *Nucl. Phys.* **B370** (1992) 3;
E. Nardi, E. Roulet and D. Tommasini, *Phys. Rev.* **D46** (1992) 3040.
[84] F. Kole et al., **HERA92**, p. 1003;
Ch. Berger et al., **HERA92**, p. 1103;
G. Ingelman and J. Rathsman, *Z. Phys.* **C60** (1993) 243.
[85] F. Boudjema et al., **HERA92**, p. 1094.
[86] K. Enqvist and I. Vilja, *Phys. Lett.* **299B** (1993) 281;
W. Buchmüller and T. Yanagida, *Phys. Lett.* **302B** (1993) 240.